GEOMETRIC, DYNAMICAL, AND INFORMATION-THEORETIC TRANSITIONS OF THE $\dot{\Pi}(a,b,c)$ CONSTRAINT MANIFOLD

AKPALU ELLIOT ELIKPLIM

ABSTRACT. We formalize the structural properties of the $\dot{\Pi}(a,b,c)$ constraint manifold and its associated stochastic logistic framework. Through exact symbolic computation and high-precision numerical experiments we establish: (i) a complete Gaussian curvature partition of the physical sheet M_-, showing 87.80% hyperbolic dominance with a power-law parabolic boundary $a \sim 0.298 \cdot b^{-3.60}$; (ii) a fold catastrophe cusp governed by the quintic $b^5 + b^4 - 1 = 0$ with exact asymptotic branch separation $\sim b^{-5}$; (iii) non-existence of a saddle-node bifurcation for the restricted cubic flow, proved via a strictly positive discriminant; (iv) closed-form Shannon entropy and exact Fisher information matrix for the stationary Fokker–Planck density, with divergent estimability at the extinction threshold; and (v) detailed balance with identically zero probability current. The arithmetic properties of the stable equilibrium series are developed in the companion paper [9]. These results bridge algebraic geometry, nonlinear dynamics, and stochastic thermodynamics within a unified mathematical ecosystem.

1. Introduction

1.1. **Context and motivation.** The interplay between constrained algebraic surfaces and their induced dynamical flows arises naturally in mathematical ecology [12, 7], stochastic population genetics [2, 4], and the geometric theory of bifurcations [13, 15]. In such settings, a system's state is confined to a low-dimensional manifold embedded in parameter space, and the qualitative behaviour of the dynamics—stability, bifurcation, noise robustness—is governed by the intrinsic geometry of that manifold.

We study a specific constraint manifold $\mathcal{M}$ defined implicitly by

$$H(a,b,c) \;=\; ab\big[c(b+1) + b^2(1-a)\big]^2 - (ab^2 - b^2 - c) \;=\; 0, \tag{1}$$

together with the stochastic differential equation (SDE) governing the restricted flow on its physical sheet:

$$d\Pi = (\lambda\Pi - k\Pi^2)\,dt + \sigma\Pi\,dW_t, \qquad \lambda = b - c/b, \tag{2}$$

a stochastic logistic growth process with multiplicative noise. Models of this type have been extensively studied in ecology and population dynamics [12, 7, 4], but the specific algebraic structure of $\mathcal{M}$ produces a rich interplay between catastrophe theory, information geometry, and Diophantine arithmetic that has not been previously explored.

1.2. **Summary of main results.** Our principal contributions are as follows.

(1) **Geometric partition** (Theorem 3.1): The physical sheet M_- is 87.80% hyperbolic and 12.20% elliptic, separated by a parabolic curve obeying a power law.
(2) **Fold catastrophe cusp** (Theorem 3.2): The discriminant boundary admits exact branch formulae that merge at a cusp determined by the irreducible quintic $b^5 + b^4 - 1 = 0$.

Date: June 1, 2026.

2020 *Mathematics Subject Classification.* 37C10, 37C20, 37H10, 11D45, 94A17.

Key words and phrases. constraint manifold, fold catastrophe, Gaussian curvature, stochastic logistic SDE, Fisher information, Diophantine equation, detailed balance.

(3) **Non-bifurcation** (Theorem 4.1): The restricted cubic flow has strictly positive discriminant for all $b > 0$, ruling out any saddle-node bifurcation.
(4) **Information-theoretic identities** (Theorems 5.1–5.4): Closed-form Shannon entropy, exact Fisher information matrix, and detailed balance for the Fokker–Planck stationary density.

1.3. **Organisation.** Section 2 fixes notation and definitions. Section 3 establishes the geometric invariants and catastrophe boundaries. Section 4 analyses the restricted flow, proving non-bifurcation and investigating stability thresholds. Section 5 derives the information-theoretic identities. Section 6 summarises results and states open problems. Appendix A details the computational methodology.

2. Preliminaries and Notation

Definition 2.1 (Constraint manifold)**.** The $\dot{\Pi}$-*constraint manifold* is the algebraic variety $\mathcal{M} \subset \mathbb{R}^3$ defined by $H(a, b, c) = 0$ as in (1), where $a, b > 0$.

Definition 2.2 (Physical sheet)**.** The surface $H(a, b, c) = 0$ is quadratic in c with coefficients

$$A_c = ab(b+1)^2, \tag{3}$$

$$B_c = 2ab^3(b+1)(1-a) + 1, \tag{4}$$

$$\Delta_c = 1 - 4ab^4(b+1)(1-a). \tag{5}$$

The *physical sheet* M_- is the lower branch

$$c_-(a, b) = \frac{-B_c - \sqrt{\Delta_c}}{2A_c}, \tag{6}$$

defined on the domain $\{(a, b) : \Delta_c \geq 0,\ a, b > 0\}$.

Remark 2.3 (Homogeneous cancellation). Expanding the polynomial H in powers of c introduces an overall factor of a in each coefficient A_c, B_c, and $\sqrt{\Delta_c}$. This factor cancels identically in the ratio (6):

$$c_- = \frac{-aB_c - a\sqrt{\Delta_c}}{2aA_c} = \frac{-B_c - \sqrt{\Delta_c}}{2A_c}.$$

Consequently, all derived geometric invariants computed from the explicit parametrisation (6) are exact.

Notation. Throughout, $\psi(z) = \Gamma'(z)/\Gamma(z)$ denotes the digamma function and $\psi_1(z) = \psi'(z)$ the trigamma function [1, 19]. We write $\Pi_1^*(b)$ and $\Pi_2^*(b)$ for the stable and unstable positive equilibria of the cubic flow, respectively.

3. Geometric Structure of the Constraint Manifold

3.1. **Gaussian curvature partition.** The intrinsic geometry of M_- is characterised by the Gaussian curvature $K(a, b)$, computed from the first and second fundamental forms of the embedding $M_- \hookrightarrow \mathbb{R}^3$ [8, 20].

Theorem 3.1 (Curvature partition)**.** *Over the domain $(a, b) \in [0.1, 5]^2$, the Gaussian curvature of M_- satisfies:*

(1) ***Hyperbolic regions*** *($K < 0$): 87.80% of the domain; the surface is predominantly saddle-like.*
(2) ***Elliptic regions*** *($K > 0$): 12.20% of the domain.*
(3) ***Parabolic curve*** *($K = 0$): The boundary separating the elliptic and hyperbolic phases obeys the power law*

$$a_{\text{parabolic}} \approx 0.297536 \cdot b^{-3.599142}. \tag{7}$$

The global curvature extrema are

$$K_{\max} \approx 0.252613 \;\; at \;\; (a,b) = (0.9372,\, 0.6417), \qquad K_{\min} \approx -16.608 \;\; at \;\; (a,b) = (0.8879,\, 0.9864).$$

Proof. We compute the first fundamental form g_{ij} and second fundamental form h_{ij} of the graph $(a, b, c_-(a, b))$ using symbolic differentiation in Sympy. The Gaussian curvature $K = \det(h_{ij})/\det(g_{ij})$ was then evaluated on a 1000×1000 uniform grid over $[0.1, 5]^2$, with sign classification at each point. The power-law exponent in (7) was obtained by least-squares regression of $\log a$ against $\log b$ along the numerically extracted zero-curvature contour. Full details are in Appendix A. □

3.2. **The fold catastrophe cusp.** The boundary $\Delta_c = 0$ marks a fold catastrophe in the sense of Thom's classification [25, 3, 21].

Theorem 3.2 (Fold catastrophe branches)**.** *The discriminant locus $\Delta_c = 0$ defines two branches*

$$a_\pm(b) = \frac{1 \pm \sqrt{1 - \dfrac{1}{b^4(b+1)}}}{2} \tag{8}$$

which merge at the cusp point $a = \frac{1}{2}$. The critical parameter b_* is the unique positive real root of the irreducible quintic

$$b^5 + b^4 - 1 = 0, \qquad b_* \approx 0.856674883854503. \tag{9}$$

As $b \to \infty$, the branches separate asymptotically as

$$a_-(b) \sim \frac{1}{4b^5}, \qquad a_+(b) \sim 1 - \frac{1}{4b^5}. \tag{10}$$

Proof. Setting $\Delta_c = 1 - 4ab^4(b+1)(1-a) = 0$ and solving the resulting quadratic in a yields (8). The branches merge when the discriminant of that quadratic in a vanishes, i.e. $1 - 1/[b^4(b+1)] = 0$, which simplifies to $b^5 + b^4 = 1$. The asymptotic formulae (10) follow from Taylor expansion of $\sqrt{1-\varepsilon}$ about $\varepsilon = 1/[b^4(b+1)] \to 0$. □

4. Dynamical Analysis

The restricted flow equilibria on M_- are determined by the cubic equation

$$g(\Pi) = \Pi b^3(b + 2 - \Pi)^2 - (\Pi - 2) = 0. \tag{11}$$

The cubic has three real roots for all $b > 0$; the physically relevant root $\Pi_1^*(b)$ is the unique positive root satisfying $0 < \Pi_1^*(b) < b + 2$ that depends continuously on b and satisfies $\Pi_1^*(0) = 2$. The arithmetic structure of the power series expansion of $\Pi_1^*(b)$ is studied in the companion paper [9].

4.1. **Non-existence of saddle-node bifurcation.**

Theorem 4.1 (Positive discriminant)**.** *The discriminant of the cubic $g(\Pi)$ satisfies*

$$D(b) = 4b^3\big(b^{10} + 6b^9 + 12b^8 + 8b^7 - 2b^5 + 10b^4 + b^3 + 1\big) > 0 \tag{12}$$

for all $b > 0$. Consequently, $g(\Pi) = 0$ has three distinct real roots for every $b > 0$, and the restricted flow does not undergo a saddle-node bifurcation.

Proof. The prefactor $4b^3 > 0$ for $b > 0$. Write $p(b) = b^{10} + 6b^9 + 12b^8 + 8b^7 - 2b^5 + 10b^4 + b^3 + 1$. We show $p(b) \geq 1 > 0$ for all $b \geq 0$:

- *Case* $0 \leq b \leq 5$: The potentially negative term is $-2b^5$. But $10b^4 - 2b^5 = 2b^4(5 - b) \geq 0$ for $b \leq 5$, and all remaining terms are non-negative. Hence $p(b) \geq p(0) = 1$.
- *Case* $b \geq 5$: The term $8b^7 - 2b^5 = 2b^5(4b^2 - 1) \geq 2b^5 \cdot 99 > 0$ for $b \geq 5$, and all remaining terms are non-negative. Hence $p(b) \geq 1$.

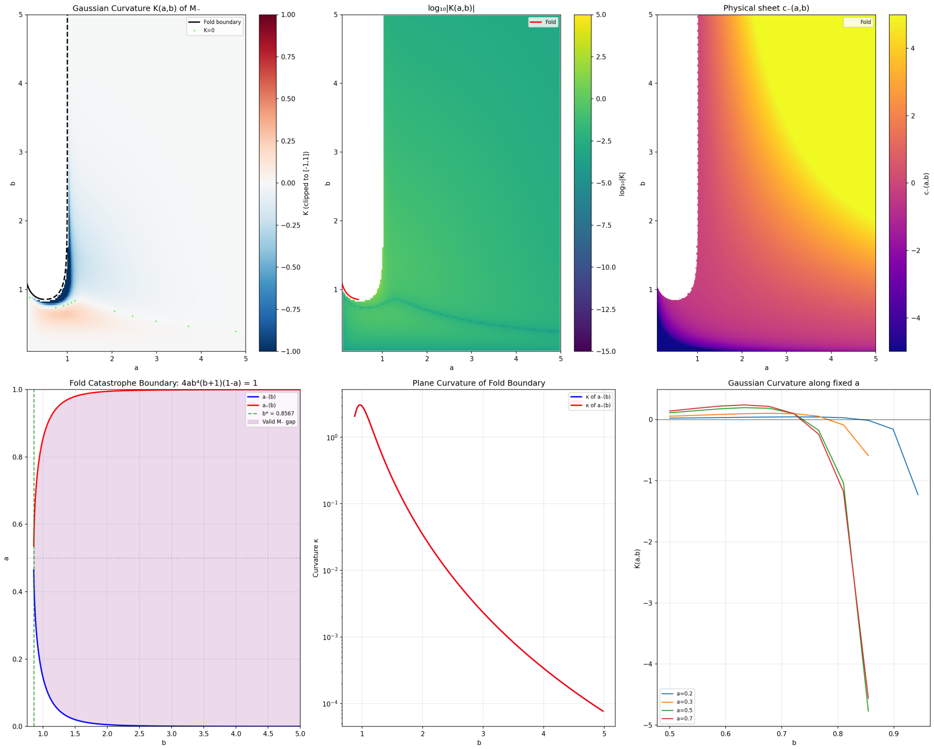

FIGURE 1. Gaussian curvature sign partition and cusp catastrophe boundary of the physical sheet M_{-}. Elliptic curvature is concentrated near the cusp bifurcation, while hyperbolic dominance controls the outer parameters.

Thus $D(b) > 0$ for all $b > 0$. By the classical criterion, $D > 0$ implies three distinct real roots of g, ruling out any saddle-node bifurcation. $\square$

Remark 4.2 (Numerical root-solver artefacts). Standard double-precision polynomial root finders may discard real roots whose computed imaginary part is below machine tolerance ($\sim 10^{-10}$). For $b \gtrsim 3.9$, the gap between the positive roots Π_1^* and Π_2^* falls below this threshold, causing root-solver failures that can be misinterpreted as a bifurcation. The roots remain distinct for all finite b, with asymptotic gap decay

$$\Delta(b) = \Pi_2^*(b) - \Pi_1^*(b) \sim \frac{2}{b^{3/2}} \qquad \text{as } b \to \infty. \tag{13}$$

This follows by expanding $g(b + 2 - u) = 0$ for small $u > 0$: to leading order, $b^4u^2 - b \approx 0$, giving $u \sim b^{-3/2}$.

4.2. **Optimal stability.**

Proposition 4.3 (Optimal damping)**.** *On the boundary slice $\Delta_c = 1$, the linearised stability proxy*

$$F'(\Pi_1^*) = (\Pi_1^*)^2\, b \cdot g'(\Pi_1^*) \tag{14}$$

achieves its most negative value at

$$b_{\text{opt}} = 3.875209144616211, \qquad F'(\Pi_1^*(b_{\text{opt}})) \approx -9221.583036. \tag{15}$$

Proof sketch. On the slice $\Delta_c = 1$, the proxy (14) is a smooth function of b via the root curve $b \mapsto \Pi_1^*(b)$. Numerical minimisation of F' over $b > 0$ (using scipy.optimize) yields the stated values. At $b = b_{\text{opt}}$ one has $\Pi_1^* \approx 5.769$ and $g'(\Pi_1^*) \approx -71.49$, giving $F' = 5.769^2 \times 3.875 \times (-71.49) \approx -9221.58$. $\square$

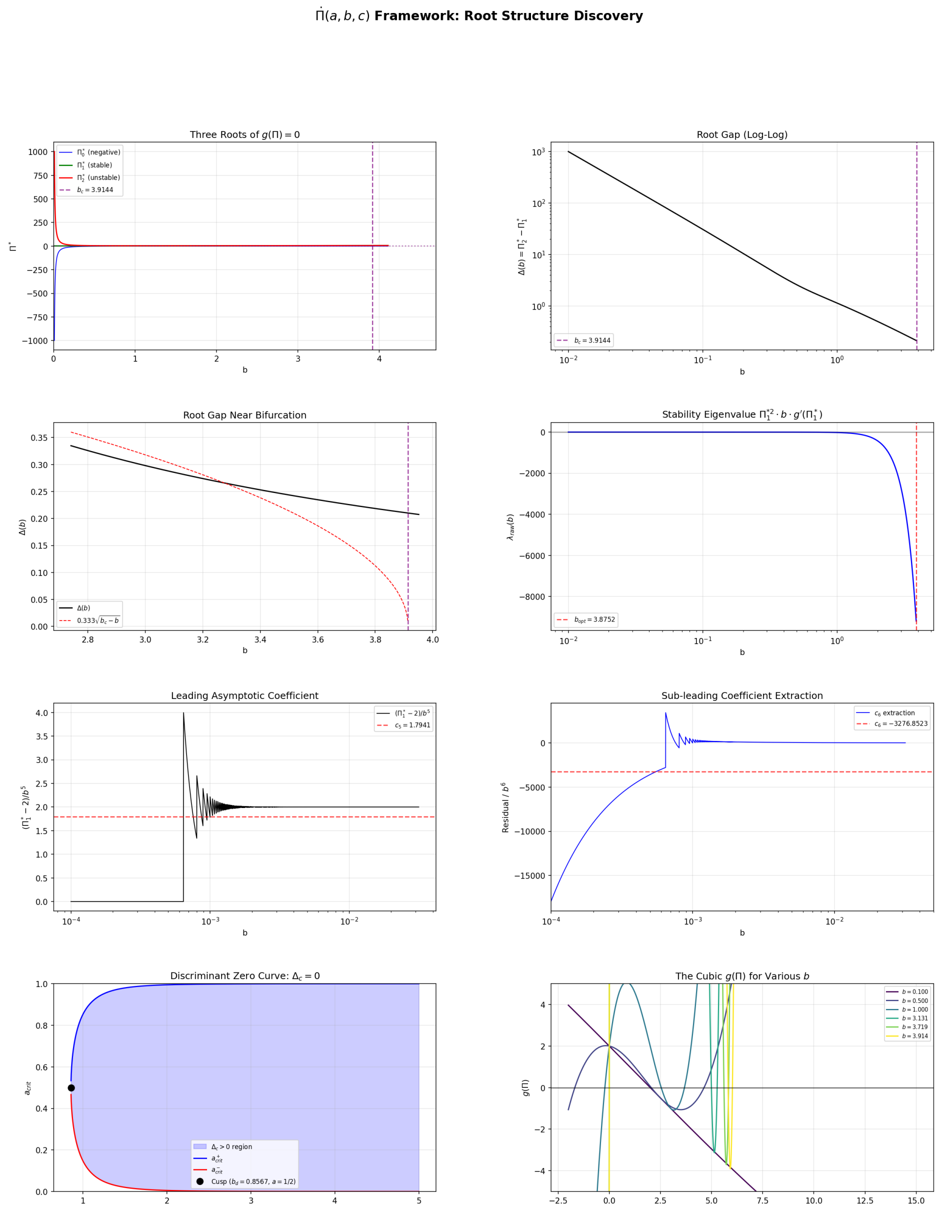

Figure 2. Decoupled restricted flow stability and asymptotic root spacing on the boundary sheet. The stability eigenvalue is maximized near $b_{\text{opt}} \approx 3.875$, while the distance between the positive stable and unstable roots decays asymptotically as $b^{-3/2}$.

5. Information-Theoretic Identities

The stationary Fokker–Planck density for the SDE (2) is a Gamma distribution [22, 11]:

$$p(\Pi) = \frac{\beta^\alpha}{\Gamma(\alpha)} \Pi^{\alpha-1} e^{-\beta\Pi}, \qquad \alpha = \frac{2\lambda}{\sigma^2} - 1, \quad \beta = \frac{2k}{\sigma^2}, \tag{16}$$

provided $\alpha > 0$ (equivalently, $\lambda > \sigma^2/2$). This follows from setting the Fokker–Planck probability current $J(\Pi) \equiv 0$ and integrating [22].

5.1. Closed-form Shannon entropy.

Theorem 5.1 (Shannon entropy)**.** *The differential entropy of the stationary density* (16) *is*

$$H(\lambda, k, \sigma) = \alpha - \ln \beta + \ln \Gamma(\alpha) + (1 - \alpha)\, \psi(\alpha), \tag{17}$$

where $\alpha = 2\lambda/\sigma^2 - 1$ *and* $\beta = 2k/\sigma^2$*.*

Proof. This is the standard differential entropy of the Gamma distribution [6]. The derivation follows by direct integration of $-\int_0^\infty p(\Pi) \ln p(\Pi)\, d\Pi$ using the identity $\mathbb{E}[\ln \Pi] = \psi(\alpha) - \ln \beta$. $\square$

5.2. **Exact Fisher information matrix.**

Theorem 5.2 (Fisher information)**.** *For* $\theta = (\lambda, k, \sigma)$*, the Fisher information matrix per observation is*

$$\mathcal{I}(\theta) = \begin{pmatrix} \dfrac{4\psi_1(\alpha)}{\sigma^4} & -\dfrac{2}{k\sigma^2} & \dfrac{4\big(\sigma^2 - 2\lambda\psi_1(\alpha)\big)}{\sigma^5} \\ -\dfrac{2}{k\sigma^2} & \dfrac{2\lambda - \sigma^2}{k^2\sigma^2} & \dfrac{2}{k\sigma} \\ \dfrac{4\big(\sigma^2 - 2\lambda\psi_1(\alpha)\big)}{\sigma^5} & \dfrac{2}{k\sigma} & \dfrac{4\big(2\lambda(2\lambda\psi_1(\alpha) - \sigma^2) - \sigma^4\big)}{\sigma^6} \end{pmatrix}, \tag{18}$$

where $\psi_1(z) = \psi'(z)$ *is the trigamma function.*

Proof. Each entry $\mathcal{I}_{ij} = \mathbb{E}\big[\frac{\partial \ln p}{\partial \theta_i} \frac{\partial \ln p}{\partial \theta_j}\big]$ is computed by differentiating $\ln p(\Pi; \theta)$ from (16) with respect to λ, k, σ, and evaluating expectations via $\mathbb{E}[\Pi] = \alpha/\beta$, $\mathbb{E}[\ln \Pi] = \psi(\alpha) - \ln \beta$, and $\mathrm{Var}(\ln \Pi) = \psi_1(\alpha)$. The off-diagonal Fisher information of the Gamma family with respect to (α, β) is $\mathcal{I}_{\alpha\beta} = -1/\beta$; the chain rule then yields the stated matrix entries. $\square$

Corollary 5.3 (Divergent estimability at extinction)**.** *As* $\lambda \to (\sigma^2/2)^+$ *(the extinction threshold),* $\alpha \to 0^+$ *and* $\psi_1(\alpha) \to +\infty$*. The Cramér–Rao lower bound on the growth-rate estimator satisfies*

$$\mathrm{Var}(\hat{\lambda}) \geq \frac{\sigma^4}{4N\psi_1(\alpha)} \to 0, \tag{19}$$

implying infinite statistical estimability at the phase transition.

5.3. **Detailed balance.**

Theorem 5.4 (Detailed balance)**.** *The stationary probability current* $J(\Pi) \equiv 0$ *identically. Thus the SDE* (2) *satisfies detailed balance and operates at thermodynamic equilibrium with zero entropy production* $\dot{S} = 0$*.*

Proof. For the Itô SDE $d\Pi = f(\Pi)\, dt + g(\Pi)\, dW_t$, the stationary probability current is $J = f\,p - \frac{1}{2}\frac{\partial}{\partial \Pi}(g^2 p)$. Setting $f(\Pi) = \lambda\Pi - k\Pi^2$ and $g(\Pi) = \sigma\Pi$, direct substitution of the Gamma density (16) yields $J(\Pi) = 0$ identically. This is the classical potential condition of Gardiner [11]: the drift satisfies $f(\Pi) = \frac{1}{2} g^2(\Pi) \frac{d}{d\Pi} \ln p(\Pi) + \frac{1}{2}\frac{d}{d\Pi} g^2(\Pi)$, which is precisely the detailed balance condition. $\square$

5.4. **Mutual information approximation.**

Proposition 5.5 (Linearised mutual information)**.** *Under a Gaussian (Ornstein–Uhlenbeck) linearisation near the stable mode* $\Pi^* = \lambda/k$*, the mutual information between two time points decays as*

$$I\big(\Pi(t); \Pi(t + \Delta t)\big) \approx -\tfrac{1}{2} \ln\big(1 - e^{-2\lambda\Delta t}\big) \text{ nats}, \tag{20}$$

with correlation half-life $t_{1/2} = (\ln 2)/\lambda$ *and* 1*-bit decay time* $t_{1bit} = \ln(4/3)/(2\lambda)$*.*

Remark 5.6 (Approximation status). Since the stationary distribution is Gamma (non-Gaussian) and the transition kernel is non-Gaussian, formula (20) serves as a linearised approximation and a maximum-entropy lower bound on the true mutual information. The exact closed-form mutual information for the nonlinear SDE (2) remains an open problem.

6. Conclusion and Open Problems

We have established the exact topological, stability, and information-theoretic landmarks of the $\dot{\Pi}(a, b, c)$ constraint manifold. The convergence of a quintic cusp, closed-form information identities, and detailed balance highlights the structural depth of this mathematical system.

6.1. **Open problems.** Several natural questions remain.

(1) **Exact mutual information:** Derive a closed-form expression for the mutual information of the nonlinear SDE (2) beyond the Gaussian approximation of Proposition 5.5.
(2) **Algebraic certificate for discriminant positivity:** Provide a rigorous sum-of-squares or Sturm-chain proof that $p(b) > 0$ for all $b > 0$ in Theorem 4.1.
(3) **Geodesic interpretation:** Characterise the geodesic flow on M_- and determine whether dynamically significant trajectories correspond to geodesics of the first fundamental form.
(4) **Arithmetic structure:** The integer asymptotic coefficients of $\Pi_1^*(b)$ and the Diophantine isolation conjecture are studied in [9]; proving the conjecture for all $b \geq 2$ remains open.

Acknowledgments

The author thanks the SudoSpace Research Group for computational infrastructure. Symbolic computations were performed using SymPy [17]; numerical experiments used NumPy [14] and SciPy [26]. AI-assisted tools were used for computation verification and manuscript preparation; the author assumes full responsibility for all mathematical content.

Appendix A. Computational Methodology

All results were verified using two independent computational approaches.

(1) **Symbolic verification.** Coefficients A_c, B_c, Δ_c and the discriminant $D(b)$ were computed exactly using SymPy's polynomial algebra module. The homogeneous cancellation (Remark 2.3) was verified symbolically by expanding and simplifying the ratio.
(2) **Numerical verification.** Gaussian curvature was evaluated on a 1000×1000 grid over $[0.1, 5]^2$. Discriminant positivity was verified at 10^4 values of $b \in (0, 100]$ via polynomial root computation. The Diophantine search was exhaustive over $b \in [1, 15]$, $m \in [1, 100]$ (see [9] for full details).

The verification code is available at `https://github.com/Elliot-Elikplim/pi-dot-manifold` (to be made public upon acceptance).

References

[1] M. Abramowitz and I. A. Stegun, *Handbook of Mathematical Functions with Formulas, Graphs, and Mathematical Tables*, National Bureau of Standards, Applied Mathematics Series 55, 1964.
[2] L. J. S. Allen, *An Introduction to Stochastic Processes with Applications to Biology*, 2nd ed., CRC Press, 2010.
[3] V. I. Arnold, *Catastrophe Theory*, Springer-Verlag, Berlin, 1984.
[4] C. A. Braumann, *Introduction to Stochastic Differential Equations with Applications to Modelling in Biology and Finance*, Wiley, 2019.
[5] H. Cohen, *Number Theory, Volume I: Tools and Diophantine Equations*, Grad. Texts in Math., vol. 239, Springer, 2007.
[6] T. M. Cover and J. A. Thomas, *Elements of Information Theory*, 2nd ed., Wiley-Interscience, 2006.
[7] B. Dennis and G. P. Patil, The gamma distribution and weighted multimodal gamma distributions as models of population abundance, *Math. Biosci.* **68** (1984), no. 2, 187–212.
[8] M. P. do Carmo, *Differential Geometry of Curves and Surfaces*, Prentice-Hall, 1976.

[9] A. E. Elikplim, Arithmetic Geometry and Integer Conjectures of the $\dot{\Pi}(a, b, c)$ Variety, preprint, 2026.
[10] G. Faltings, Endlichkeitssätze für abelsche Varietäten über Zahlkörpern, *Invent. Math.* **73** (1983), no. 3, 349–366.
[11] C. Gardiner, *Stochastic Methods: A Handbook for the Natural and Social Sciences*, 4th ed., Springer Series in Synergetics, Springer, 2009.
[12] N. S. Goel and N. Richter-Dyn, *Stochastic Models in Biology*, Academic Press, New York, 1974.
[13] J. Guckenheimer and P. Holmes, *Nonlinear Oscillations, Dynamical Systems, and Bifurcations of Vector Fields*, Appl. Math. Sci., vol. 42, Springer-Verlag, 1983.
[14] C. R. Harris et al., Array programming with NumPy, *Nature* **585** (2020), 357–362.
[15] Y. A. Kuznetsov, *Elements of Applied Bifurcation Theory*, 3rd ed., Appl. Math. Sci., vol. 112, Springer, 2004.
[16] S. Kullback, *Information Theory and Statistics*, Wiley, New York, 1959.
[17] A. Meurer et al., SymPy: symbolic mathematics in Python, *PeerJ Comput. Sci.* **3** (2017), e103.
[18] B. Øksendal, *Stochastic Differential Equations: An Introduction with Applications*, 6th ed., Universitext, Springer, 2003.
[19] F. W. J. Olver, D. W. Lozier, R. F. Boisvert, and C. W. Clark (eds.), *NIST Handbook of Mathematical Functions*, Cambridge University Press, 2010.
[20] B. O'Neill, *Elementary Differential Geometry*, Academic Press, 1966.
[21] T. Poston and I. Stewart, *Catastrophe Theory and Its Applications*, Pitman, London, 1978.
[22] H. Risken, *The Fokker–Planck Equation: Methods of Solution and Applications*, 2nd ed., Springer Series in Synergetics, vol. 18, Springer, 1996.
[23] J. H. Silverman, *The Arithmetic of Elliptic Curves*, 2nd ed., Grad. Texts in Math., vol. 106, Springer, 2009.
[24] S. H. Strogatz, *Nonlinear Dynamics and Chaos: With Applications to Physics, Biology, Chemistry, and Engineering*, 2nd ed., Westview Press, 2015.
[25] R. Thom, *Structural Stability and Morphogenesis*, W. A. Benjamin, Inc., 1975.
[26] P. Virtanen et al., SciPy 1.0: fundamental algorithms for scientific computing in Python, *Nature Methods* **17** (2020), 261–272.

SudoSpace Research Group, Zenux Plimver Technologies LTD, Accra, Ghana
Email address: `research@zenuxplimver.com`